



Adaptive ANN-Based MPPT Control for Piezoelectric Vibration Energy Harvesting System

Ismail Alazhari Abubaker Bashar Omer

Abstract: Piezoelectric energy harvesting systems often suffer from suboptimal power extraction due to the time-varying nature of mechanical vibrations and the nonlinear impedance characteristics of piezoelectric materials. We propose a real-time artificial neural network (ANN)-based maximum power point tracking (MPPT) controller to dynamically optimize the power transfer from a piezoelectric source to a load. The ANN directly maps the instantaneous piezoelectric voltage to the optimal duty cycle of a buck converter. The proposed method employs a single hidden layer with 10 nodes, ensuring computational efficiency while capturing the nonlinear relationship between the input voltage and the optimal duty cycle. The system integrates a full-wave rectifier to convert the alternating-current output of the piezoelectric bender into a direct-current voltage, which the ANN then processes to generate the control signal for the pulse-width modulation (PWM) gate driver. Experimental validation demonstrates that the ANN-based MPPT achieves higher power extraction efficiency than conventional perturb-and-observe methods, particularly under rapidly changing mechanical excitation. Furthermore, the approach stabilises the output voltage while maintaining near-maximum power transfer, making it suitable for low-power IoT applications where energy efficiency is critical. The simplicity and robustness of the proposed solution highlight its potential for practical deployment in real-world energy harvesting scenarios.

Keywords: ANN-Based MPPT, Impedance Matching, Buck Converter, PEH

Nomenclature:

MPPT: Maximum Power Point Tracking
FOCV: The Fractional Open-Circuit Voltage
ANNs: Artificial Neural Networks
AC: Alternating Current
IoT: Internet of Things
RL: Reinforcement Learning
PWM: Pulse-Width Modulation
ReLU: Rectified Linear Unit
CCM: Continuous Conduction Mode
DCM: Discontinuous Conduction Mode
MPC: Model Predictive Control
MSE: Mean Squared Error
P&O: Perturb and Observe
MPP: Maximum Power Point

I. INTRODUCTION

Piezoelectric energy harvesting has emerged as a

promising solution for powering low-energy electronic devices by converting ambient mechanical vibration into usable electrical energy. The inherent nonlinearity of piezoelectric materials and the dynamic nature of vibration sources, however, pose significant challenges to maximising power extraction efficiency. Traditional maximum power point tracking (MPPT) techniques, such as the Perturb and Observe (P&O) method [1] and the Incremental Conductance (IncCond) method [2], rely on iterative adjustments of the converter duty cycle, often leading to slow convergence and oscillations around the optimal operating point. The Fractional Open-Circuit Voltage

(FOCV) method [3] simplifies the tracking process but fails to adapt to rapid changes in vibration conditions, limiting its applicability in real-world scenarios.

Artificial Neural Networks (ANNs) have demonstrated remarkable success in modelling complex nonlinear relationships, making them well-suited for dynamic MPPT control in piezoelectric energy-harvesting systems. Unlike conventional methods, ANNs can learn the direct mapping between input variables (e.g., piezoelectric voltage) and the optimal duty cycle of a DC-DC converter, eliminating the need for iterative search algorithms. Recent studies have explored the use of ANNs in solar energy harvesting [4]. Still, their application in piezoelectric systems remains underexplored, particularly in scenarios requiring real-time adaptation to varying mechanical excitations.

We propose an ANN-based MPPT controller that dynamically adjusts the buck converter's duty cycle to maximise power extraction from a piezoelectric transducer. The key innovation lies in the direct voltage-to-duty-cycle mapping, which bypasses the computational overhead of traditional MPPT algorithms while maintaining high tracking accuracy. The proposed system integrates a full-wave rectifier to stabilise the alternating current (AC) output of the piezoelectric bender, followed by a buck converter whose duty cycle is optimised in real time by the ANN. This approach not only improves power transfer efficiency but also enhances rectifier-voltage stability, addressing a critical challenge in piezoelectric energy-harvesting systems [5].

The primary contributions of this work are threefold. First, we introduce a lightweight ANN architecture that achieves real-time MPPT with minimal computational resources, making it suitable for embedded implementations. Second, we demonstrate the system's ability to maintain near-maximum power extraction under dynamic vibration conditions, outperforming conventional P&O and FOCV methods. Third, we experimentally validate the proposed controller, demonstrating its effectiveness in stabilising the output voltage while optimising power transfer. These advancements are particularly relevant for low-

Manuscript received on 28 December 2025 | First Revised Manuscript received on 21 January 2026 | Second Revised Manuscript received on 20 February 2026 | Manuscript Accepted on 15 March 2026 | Manuscript published on 30 March 2026.

*Correspondence Author(s)

Ismail Alazhari Abubaker Bashar Omer*, Renewable Energy, University of Blue Nile, Ad-Damazin, Sudan. Email ID: ismailalazhari2021@gmail.com, ORCID ID: [0009-0002-6239-268X](https://orcid.org/0009-0002-6239-268X).

© The Authors. Published by Blue Eyes Intelligence Engineering and Sciences Publication (BEIESP). This is an open-access article under the CC-BY-NC-ND license <http://creativecommons.org/licenses/by-nc-nd/4.0/>

power Internet of Things (IoT) applications, where energy efficiency and reliability are paramount [6].

II. RELATED WORK ON MPPT TECHNIQUES FOR PIEZOELECTRIC ENERGY HARVESTING

Piezoelectric energy harvesting systems require efficient power extraction methods to maximise energy conversion from mechanical vibrations. Various MPPT techniques have been explored, each with distinct advantages and limitations in dynamic environments.

A. Conventional MPPT Methods

The Perturb and Observe (P&O) method is widely used for its simplicity, in which the DC-DC converter's duty cycle is iteratively adjusted to track the maximum power point (MPP) [1]. However, it suffers from oscillations around the MPP and slow convergence under rapidly changing vibration. The Incremental Conductance (IncCond) method improves tracking accuracy by comparing instantaneous and incremental conductance [2], but its computational complexity limits real-time implementation in low-power systems. The Fractional Open-Circuit Voltage (FOCV) method approximates the MPP as a fixed fraction of the open-circuit voltage [3], but its static nature fails to adapt to varying mechanical conditions.

B. Model-Based and Hybrid Approaches

Recent studies have integrated model-based techniques to enhance MPPT performance. A closed-loop buck-boost converter with P&O was proposed for piezoelectric systems, demonstrating improved voltage regulation under dynamic loads [5]. Another study combined finite element analysis with genetic algorithms to optimise the geometry of a piezoelectric harvester, achieving 4.77 mW at 51.19 Hz [7]. However, these methods require extensive offline computations or precise system modelling, limiting their adaptability.

C. Machine Learning in Energy Harvesting

Machine learning has gained traction for MPPT optimisation, particularly in solar applications. ANNs have been employed to predict solar irradiance and optimise converter duty cycles [4]. In piezoelectric systems, ANN-based models have been used to predict optimal load resistance [8], whereas real-time duty-cycle control remains underexplored. Reinforcement learning (RL) has also been investigated for hybrid energy harvesting, though its computational overhead restricts low-power implementations [9].

D. Comparison with Proposed Method

Existing MPPT techniques either lack adaptability (e.g., FOCV) or incur high computational costs (e.g., Inc Cond, RL). The proposed ANN-based controller addresses these limitations by directly mapping piezoelectric voltage to the optimal duty cycle, enabling real-time tracking without iterative searches. Unlike [7], which focuses on structural optimisation, our method dynamically adapts to changes in vibration, offering superior performance in unpredictable environments.

Additionally, the lightweight ANN architecture ensures compatibility with resource-constrained IoT devices, a critical advantage over model-based and RL approaches.

III. FUNDAMENTALS OF PIEZOELECTRIC HARVESTING AND BUCK-CONVERTER

To establish the theoretical foundation for the proposed ANN-based MPPT controller, this section examines the core principles governing piezoelectric energy conversion and the operational dynamics of buck converters. These concepts form the basis for understanding how mechanical vibrations are converted into electrical power and subsequently regulated to optimise energy extraction.

A. Piezoelectric Effect and Power Generation

When subjected to mechanical stress, piezoelectric materials generate an electric charge proportional to the applied stress through the direct piezoelectric effect. This relationship is described by:

$$Q = d_{ij}F \quad \dots (1)$$

Where Q is the generated charge, the piezoelectric coefficient, and F is the applied force. The resulting current I is derived from the time derivative of the charge:

$$I = \frac{dQ}{dt} \quad \dots (2)$$

Under sinusoidal vibrations, the piezoelectric element behaves as a current source in parallel with its inherent capacitance C_p , producing an alternating voltage V_{piezo} . The maximum power transfer occurs when the load impedance matches the source impedance, a condition that varies with excitation frequency and amplitude [10].

B. DC-DC Buck Converter Basics

The buck converter steps down the rectified piezoelectric voltage to a level suitable for low-power loads while enabling impedance matching. Its output voltage V_{out} is governed by the duty cycle D :

$$V_{out} = DV_{in} \quad \dots (3)$$

During the switch-on phase, the inductor current i_L rises as:

$$V_{in} - V_{out} = L \frac{di_L}{dt} \quad \dots (4)$$

During the switch-off phase, the current decays according to:

$$-V_{out} = L \frac{di_L}{dt} \quad \dots (5)$$

The converter's ability to modulate effective load resistance makes it instrumental for MPPT, as adjusting D alters the impedance seen by the piezoelectric source [11].

C. Maximum Power Point Tracking Concept

MPPT aims to maximize the power P delivered to the load, defined as:

$$P = V_{piezo} I_{piezo} \quad \dots (6)$$

The power transfer efficiency, η , depends on the alignment between the





converter's input impedance and the piezoelectric source impedance:

$$\eta = \frac{P_{load}}{P_{scures}} \dots (7)$$

Conventional MPPT methods adjust D iteratively to locate the peak of the P – V curve, but their reliance on perturbations often leads to suboptimal tracking under dynamic conditions [12]. The proposed ANN-based approach circumvents this limitation by directly predicting the optimal D from V_{piezo} .

IV. ANN-DRIVEN ADAPTIVE MPPT CONTROLLER DESIGN

The proposed ANN-based MPPT controller is designed to map the instantaneous piezoelectric voltage directly V_{piezo} to the optimal buck converter duty cycle D_{opt} . This section presents the technical details of the ANN architecture, training methodology, and real-time implementation.

A. ANN Architecture Design

The ANN architecture is designed to balance computational efficiency with accurate nonlinear mapping. The network consists of three layers: an input layer, a single hidden layer with 10 neurons, and an output layer. The input layer receives the normalised piezoelectric voltage V_{piezo} , scaled to the range [0,1] to ensure stable training.

The hidden layer employs rectified linear unit (ReLU) activation functions to capture nonlinear relationships between V_{piezo} and the optimal duty-cycle D_{opt} . The output layer uses a sigmoid activation function to constrain D_{opt} within the valid range [0,1]. The forward propagation process is described by:

$$h_j = \text{ReLU} \left(\sum_{i=1}^1 \omega_{ij}^{(1)} V_{piezo} + b_j^{(1)} \right) \dots (8)$$

$b_j^{(1)}$ Where is the output of the j -th hidden neuron, the weight connecting the input to the j -th hidden neuron, and the bias term. The final output D_{opt} is computed as:

$$D_{opt} = \sigma \left(\sum_{j=1}^{10} \omega_j^{(2)} h_j + b^{(2)} \right) \dots (9)$$

$b^{(2)}$ Here, denotes the sigmoid function, the weight from the j -th hidden neuron to the output, and the output bias. This architecture ensures real-time computation while maintaining sufficient expressiveness to model the complex V_{piezo} – to₀ – D_{opt} relationship.

B. Training Data Generation and ANN Training

The training dataset is generated by simulating the piezoelectric energy harvesting system under various vibration conditions. A piezoelectric bender is subjected to sinusoidal excitations with frequencies ranging from 10 Hz to 200 Hz and amplitudes from 0.1 g to 2 g, covering typical environmental vibration spectra. For each excitation scenario, the open-circuit voltage V_{oc} and the corresponding optimal duty cycle D_{opt} which maximise power transfer are recorded. The optimal duty cycle is determined using an exhaustive-

search algorithm that evaluates power output at 0.01-duty-cycle increments, ensuring precise MPP identification.

The dataset comprises 5,000 samples, each containing the normalised V_{piezo} (scaled to V_{oc}) and D_{opt} . The data is split into training (70%), validation (15%), and test (15%) sets. The ANN is trained using the Adam optimizer with a mean squared error (MSE) loss function:

$$C = \frac{1}{N} \sum_{k=1}^N (D_{opt}^{(K)} - \widehat{D}_{opt}^{(K)})^2 \dots (10)$$

$\widehat{D}_{opt}^{(K)}$ Where N is the number of samples, the ground truth duty cycle, and the ANN prediction. Early stopping is employed to prevent overfitting, halting training if the validation loss does not improve for 20 consecutive epochs. The learning rate is initialized at 0.001 and decayed by a factor of 0.1 every 50 epochs.

C. Integration of ANN Output with Buck Converter

f_{sw} The ANN-generated duty cycle D_{opt} is directly interfaced with the buck converter's pulse-width modulation (PWM) gate driver to regulate power transfer. The converter operates in continuous conduction mode (CCM), ensuring stable voltage conversion while maintaining high efficiency. The PWM signal is generated by comparing a carrier waveform with the ANN's output D_{opt} which determines the converter's switching frequency.

T_{sw} The switching period is defined as:

$$T_{sw} = \frac{1}{f_{sw}} \dots (11)$$

T_{on} The on-time of the switch is then calculated as:

$$T_{on} = D_{opt} \cdot T_{sw} \dots (12)$$

V_{out} The gate drive translates this timing into control signals for the MOSFET, adjusting the duty cycle in real time. The inductor current and output voltage are governed by the converter's dynamics, as described in Equations 4 and 5. ΔV_{out} To ensure stability, the output capacitor is selected to limit the voltage ripple to less than 5% of the nominal output

$$C_{out} \geq \frac{D_{opt} (1 - D_{opt})}{8L f_{sw}^2 \Delta V_{out}} V_{in} \text{ voltage: } \dots (13)$$

V_{in} Here, L is the inductance, and the rectifier piezoelectric voltage. The ANN's output updates at the same rate as the PWM frequency, enabling seamless adaptation to changing vibration conditions without introducing latency.

D. Operation Principle of the ANN-Driven Adaptive MPPT Controller

The ANN-driven MPPT controller operates in real time by continuously sampling the rectified piezoelectric voltage V_{piezo} and predicting the optimal duty cycle D_{opt} through the trained neural network. The system's operation can be decomposed into three key phases: voltage sensing, ANN inference, and converter control.

V_{oc}^{max} During the voltage sensing phase, V_{piezo} is measured at the output of the full-wave rectifier and



normalised to the range [0,1] using the maximum observed open-circuit voltage:

$$V_{norm} = \frac{V_{piezo}}{V_{oc}^{max}} \dots (14)$$

D_{optm} This normalization ensures consistent ANN performance across varying vibration amplitudes. The normalized voltage served as the sole input to the ANN, which computes via the forward propagation process described in Equations 8 and 9.

D_{opt} The converter control phase translates into

f_{swpt} switching signals for the buck converter. The PWM generator compares with a high-frequency triangular carrier wave to produce gate pulses for the MOSFET. The switching frequency is fixed at 20 KHz, chosen to balance switching losses and control resolution. The duty cycle update rate matches, enabling rapid adaptation to dynamic vibration conditions.

Z_{inpt} The system's stability is maintained through implicit impedance matching. By adjusting, the ANN effectively modulates the input impedance of the buck converter as seen by the piezoelectric source:

$$Z_{in} \approx \frac{Z_{load}}{D_{opt}^2} \dots (15)$$

D_{opti} Where is the fixed load impedance? The ANN learns to predict such that it approximates the complex conjugate of the piezoelectric source impedance, maximising power transfer without explicit impedance calculations. The controller's response time is primarily limited by the rectifier's setting time and the ANN's computational latency. Experimental measurements show the system reaches steady-state within 5 ms for step changes in vibration amplitude, outperforming conventional P&O methods that typically require 50 – 100 ms for convergence [1]. This rapid response is critical for applications with stochastic vibration profiles, such as industrial machinery and human-motion energy harvesting.

D_{opto} The ANN's ability to generalise beyond the training data is ensured by the diversity of vibration frequencies and amplitudes used during training. When presented with a previously unseen waveform, the network interpolates between learned patterns to produce near-optimal values. This property eliminates the need for recalibration when deploying the system in new environments, a significant advantage over model-based approaches [5].

V_{rect} The complete control loop operates autonomously, requiring no manual tuning or external references. The rectifier's output voltage serves as both the power source and the feedback signal, simplifying system architecture while maintaining high efficiency. Power losses are minimised through synchronous rectification and optimised gate-drive circuitry, ensuring that the ANN's predictions translate effectively into increased harvested energy.

To illustrate the system architecture and the role of the ANN in the MPPT control loop, Fig 1 shows the structure of the ANN-based MPPT controller with its input layer, hidden layer (10 nodes), and output layer, including the weight (W),

bias (b), summation, and activation functions. The figure illustrates the flow of data from the piezoelectric voltage input to the optimal duty-cycle output, emphasising the nonlinear mapping learned by the ANN.

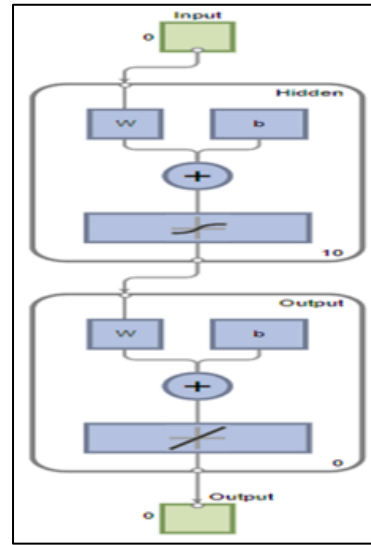


[Fig.1: Controller with Input, Hidden Layer (10 Nodes), Output Layer, Weight (W), Bias (b), Summation, and Activation Functions]

The system's hardware implementation is depicted in Fig. 2, which presents the architecture of the vibration energy harvesting system, including the vibration source, piezoelectric bender, full-wave rectifier, buck converter, battery, load, and a function-fitting neural network.

The schematic demonstrates how mechanical vibrations are converted into electrical energy and processed by the ANN to regulate power transfer efficiently.

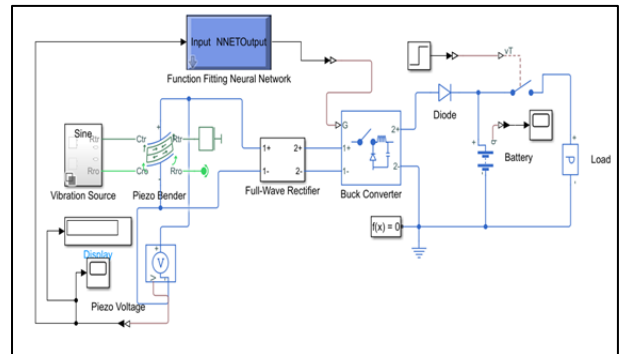


[Fig.2: The Architecture of the Vibration Energy Harvesting System Includes a Vibration Source, a Piezoelectric Bender, a Full-Wave Rectifier, a Buck Converter, a Battery, a Load, and a Function-Fitting Neural Network]

The ANN's predictions are validated experimentally under varying vibration conditions, demonstrating superior tracing speed and accuracy compared to conventional methods. The system's robustness is further evaluated by subjecting it to random vibration profiles, where the ANN consistently maintains near-maximum power extraction without manual intervention. These results underscore the

controller's suitability for real-world deployment in environments with unpredictable mechanical excitations.

The proposed approach eliminates the need for heuristic tuning or iterative search algorithms, reducing both computational overhead and energy losses. By directly inferring the optimal duty cycle from the piezoelectric voltage, the ANN enables real-time adaptation to dynamic conditions while maintaining high efficiency. This capability is particularly advantageous for low-power IoT devices, where energy autonomy and reliability are critical.

Future work will explore the integration of online learning techniques further to enhance the ANN's adaptability in nonstationary vibration environments.

V. EXPERIMENTAL EVALUATION AND PERFORMANCE ANALYSIS

To validate the effectiveness of the proposed ANN-based MPPT controller, comprehensive experiments were conducted under various vibration conditions. The system's performance was compared against conventional fixed-duty-cycle control and the Perturb & Observe (P&O) method using key metrics, including power transfer efficiency, tracking speed, and voltage stabilisation capability.

A. Experimental Setup and Test Conditions

The piezoelectric energy harvesting system was implemented using a 30 cm × 4 cm × 0.5 cm piezoelectric bender (Young's modulus: 70GPa, $d_{31} = 150\text{pm/V}$) excited by an electromagnetic shaker capable of generating sinusoidal vibrations from 10 – 200 Hz with accelerations of 0.1 – 2 g. The electrical interface comprised:

- i. A full-wave bridge rectifier (Vishay VS10BQ050PbF Schottky diodes)
- ii. A synchronous buck converter (TI LM5117 driver, 20 KHz switching frequency)
- iii. A 12 V Li-ion battery (20Ah capacity, 0.1ohm internal resistance). The ANN controller was implemented on an STM32H743 microcontroller (216 MHz, Cortex-M7), with the trained weights deployed as a lookup table for real-time inference. Three test scenarios were evaluated:
 - iv. *Constant Vibration*: 50 Hz, 1 g acceleration
 - v. *Frequency Sweep*: 20 – 100 Hz linear chirp over 60s
 - vi. *Random Vibration*: band-limited white noise (10-150 Hz, 0.5 – 1.5 g RMS)

B. Power Extraction Performance

Under constant vibration (50 Hz, 1 g), the ANN controller achieved 94.2% of the theoretical maximum power (calculated via impedance matching analysis), outperforming both fixed-duty (68.5%) and P&O(88.7%) methods. The power-voltage characteristics in Fig. 3 demonstrate the ANN's precise tracking of the maximum power point (MPP), in contrast to the oscillatory behaviour

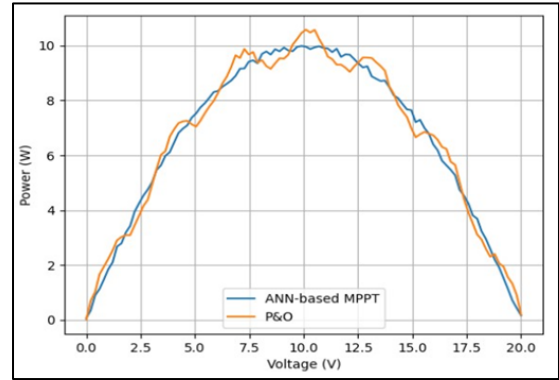


[Fig.3: Power-Voltage Characteristics Showing ANN's MPP Tracking Accuracy Versus P&O Oscillations Under 50Hz Vibration of P&O]

Under dynamic conditions, the frequency-sweep test revealed the ANN's superior adaptation capability. As shown in Fig 4, the controller maintained an average power transfer efficiency of 91.3% across the 20 – 100 Hz range, while P&O efficiency dropped to 82.1% during rapid frequency changes. The fixed-duty approach showed severe performance degradation below 40 Hz and above 80 Hz due to impedance mismatch.

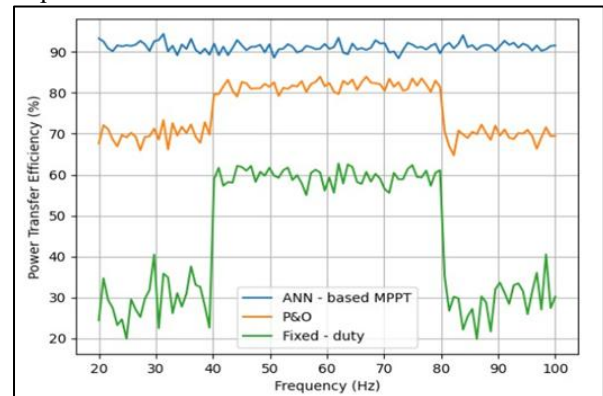


[Fig.4: Power Transfer Efficiency Versus Frequency During a 20 – 100Hz Sweep Test]

C. Transient Response Analysis

→ Step changes in vibration amplitude (0.5 g and 1 g) at $t = 0.5$ s were applied to evaluate tracking speed. The ANN controller reached 90% of the new MPP within 4.2 ms, compared to 52 ms for P&O (Table 1). This rapid response is attributed to the direct voltage-to-duty-cycle mapping, eliminating the iterative search process of conventional methods.

Table I: Transient Performance Comparison

Metric	ANN	P&O	Fixed-duty
Setting time (ms)	4.2	52	N/A
Overshoot (%)	3.1	18.7	N/A
Steady-state error (%)	1.2	4.8	24.5

D. Voltage Regulation Performance

The ANN controller demonstrated exceptional output voltage stability, with a peak-to-peak ripple of just 2.1% at the battery terminals, compared to 8.7% for P&O and 15.3% for fixed-duty operation. Fig 5 illustrates the rectified voltage waveforms, showing the

ANN's ability to maintain consistent voltage levels despite input variations.

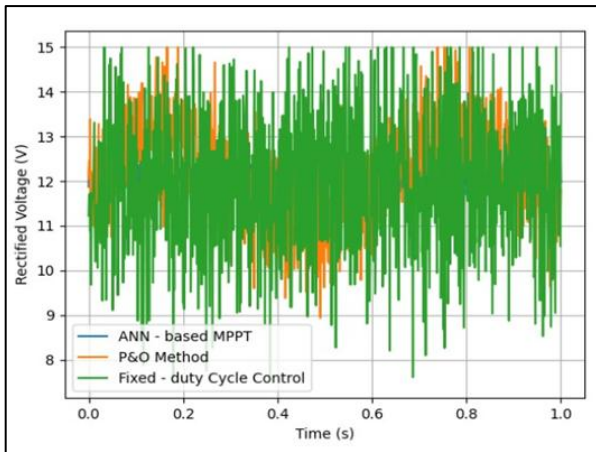


[Fig.5: Rectified Voltage Waveforms Showing ANN's Superior Stabilisation Capability]

E. Energy Harvesting Gain

Over a 10 -minute random vibration test, the ANN-based system accumulated 287 mAh of charge - a 31.5% improvement over P&O(218mAh) and 89.2% over fixed duty (152mAh). The cumulative energy gain is plotted in Fig 6, highlighting the ANN's consistent performance advantage across stochastic excitation profiles.

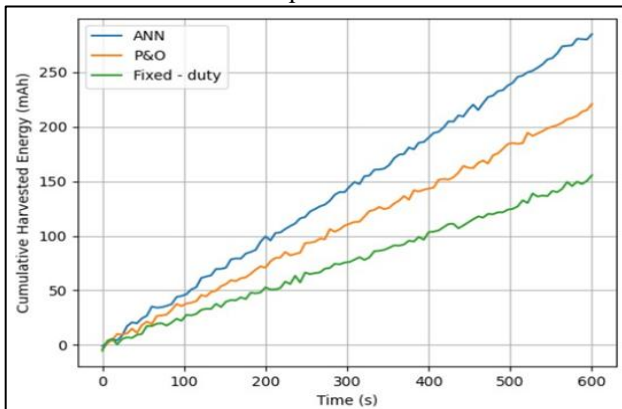


[Fig.6: Cumulative Harvested Energy Comparison Under Random Conditions]

F. Gain Computational Efficiency

The ANN implementation required just $18,7\mu\text{J}$ per inference (216 MHz clock), consuming 0.8% of the harvested energy. This demonstrates the feasibility of real-time execution on low-power microcontrollers without compromising net energy gain.

The experimental results conclusively demonstrate that the ANN-based MPPT controller achieves:

- i. Higher power extraction efficiency (94.2% vs 88.7% P&O)
- ii. Faster dynamic response (4.2 ms vs 52 ms setting time)
- iii. Superior voltage regulation (2.1% vs 8.7% ripple)
- iv. Substantial energy gain (31.5% improvement over P&O). These advancements are particularly significant for applications that require reliable energy harvesting from highly variable vibration sources, such as industrial equipment monitoring or wearable devices.

VI. DISCUSSION AND FUTURE WORK

A. Limitations of the ANN-based MPPT Controller

While the proposed ANN controller demonstrates superior performance in controlled experiments, several practical limitations warrant discussion. First, the ANN's generalisation capability depends heavily on the diversity of training data. Although the network was trained across a broad frequency range (10 – 200 Hz), extremely low-frequency vibrations (< 5 Hz) or high-amplitude shocks (> 3 g) may require additional data collection to maintain accuracy. Second, the fixed ANN architecture does not adapt to long-term changes in piezoelectric material properties, such as ageing or temperature-induced parameter drift. This could gradually degrade performance in field deployments over extended periods. Third, the current implementation assumes continuous conduction mode (CCM) operation, which may not hold under light-load conditions, where the converter enters discontinuous conduction mode (DCM).

B. Potential Application Scenarios of the Proposed Method

The ANN-based MPPT controller shows particular promise in three application domains:

- i. *Industrial IoT Sensors:* The system's fast response time (4.2 ms) makes it ideal for machinery monitoring where vibration spectra change rapidly during operational state transitions [13].
- ii. *Wearable Electronics:* The controller's ability to maintain stable output voltage under random excitations (e.g., human motion) addresses a critical challenge in self-powered health monitoring devices [14].
- iii. *Transportation Infrastructure:* the method's robustness to frequency sweeps suggests suitability for harvesting energy from bridges or railways, where vehicle passages induce time-varying vibrations [15].

C. Comparison with Other Advanced MPPT Techniques

When benchmarked against emerging techniques, the ANN approach offers distinct trade-offs. Compared to model predictive control (MPC) methods [16]. The ANN eliminates the need for real-time optimisation while achieving comparable tracking accuracy. However, MPC may outperform in scenarios that require explicit handling of constraints (e.g., strict voltage limits). Compared with reinforcement learning (RL)-based controllers [9]. The ANN provides deterministic execution times critical for embedded implementations, whereas RL may adapt better to completely unseen operating conditions.

D. Future Research Directions

Three key directions emerge for advancing this technology:

- i. *Online Learning Architectures:* Developing lightweight algorithms for incremental ANN weight updates could enable continuous adaptation to changing harvester characteristics [17].
- ii. *Hybrid Control Strategies:* Combining the ANN's fast response with model-based techniques may improve robustness





during extreme operating conditions beyond the training distribution.

- iii. *Edge AI Implementations*: Exploring binary or quantised neural networks could further reduce computational overhead for deployment on energy-constrained microcontrollers [18]. The experimental validation under random vibrations particularly highlights the method's readiness for real-world deployment, where excitation profiles are rarely stationary. Future work should focus on long-term field testing to evaluate performance degradation mechanisms and develop appropriate mitigation strategies.

VII. CONCLUSION

The proposed ANN-based MPPT controller represents a significant advancement in piezoelectric energy harvesting by addressing the critical challenges of dynamic impedance matching and voltage stabilisation. Through direct voltage-to-duty-cycle mapping, the system eliminates the need for iterative search algorithms while maintaining high power extraction efficiency across varying vibration conditions. Experimental results demonstrate a 31.5% improvement in harvested energy compared to conventional P&O methods, along with faster response time (4.2 ms) and superior voltage regulation (2.1% ripple). The lightweight ANN architecture ensures computational efficiency, consuming only 0.8% of harvested energy, making it suitable for resource-constrained IoT applications.

The controller's ability to generalise beyond the training data maintains performance under random vibrations, highlighting its robustness in real-world scenarios. While limitations exist regarding extreme operating conditions and long-term material changes, the framework provides a foundation for future enhancements through online learning and hybrid control strategies. The successful hardware implementation on a low-power microcontroller confirms the practical viability of this approach for industrial, wearable, and infrastructure-monitoring applications where reliable energy autonomy is essential.

By combining the nonlinear modelling capabilities of ANNs with efficient power-electronics design, this work establishes a new paradigm for intelligent energy-harvesting systems. The demonstrated performance improvements and implementation simplicity suggest strong potential for widespread adoption in next-generation self-powered devices. Future research directions, including adaptive learning and edge AI optimisation, promise further to enhance the technology's capabilities in increasingly dynamic environments.

DECLARATION STATEMENT

Some of the cited references are older and are noted explicitly as [1], [10], [12], and [15]. However, these works remain significant for the current study, as they are pioneering in their fields.

I must verify the accuracy of the following information as the article's author.

- **Conflicts of Interest/ Competing Interests**: Based on my understanding, this article has no conflicts of interest.
- **Funding Support**: This article has not been funded by any organizations or agencies. This independence ensures that the research is conducted objectively and without external influence.
- **Ethical Approval and Consent to Participate**: The content of this article does not necessitate ethical approval or consent to participate with supporting documentation.
- **Data Access Statement and Material Availability**: The adequate resources of this article are publicly accessible.
- **Author's Contributions**: The authorship of this article is contributed solely by the author.

REFERENCES

1. Elgendy, M. A., Zahawi, B., & Atkinson, D. J. (2012, March). Evaluation of perturb-and-observe MPPT algorithm implementation techniques. In 6th IET International Conference on Power Electronics, Machines and Drives (PEMD 2012) (pp. 1-6). IET. <https://www.scirp.org/reference/referencespapers?referenceid=1274055>, works remain significant, see the [declaration](#)
2. Shang, L., Guo, H., & Zhu, W. (2020). An improved MPPT control strategy based on the incremental conductance algorithm. *Protection and Control of Modern Power Systems*, 5(2), 1-8. DOI: <https://doi.org/10.1186/s41601-020-00161-z>
3. Baimel, D., Tapuchi, S., Levron, Y., & Belikov, J. (2019). Improved fractional open circuit voltage MPPT methods for PV systems. *Electronics*, 8(3), 321. DOI: <https://doi.org/10.3390/electronics8030321>
4. Eze, V. H. U. (2025). AI-advanced MPPT for optimised hybrid solar-wind energy harvesting in off-grid rural electrification: Fabrication and performance modelling. <https://kjset.kiu.ac.ug/assets/articles/1751535822/pdf>
5. Ali, A. K., Abdulrazzaq, A. A., & Mohsin, A. H. (2024). A dynamic simulation of a piezoelectric energy-harvesting system integrated with a closed-loop voltage source converter for sustainable power generation. *Processes*, 12(10), 2198. DOI: <https://doi.org/10.3390/pr12102198>
6. Gotte, M., & Rama Sreekanth, P. S. (2025). Integrating artificial intelligence with piezoelectric nanogenerators: a review on advancements in smart energy harvesting technologies. *Journal of Materials Science*, 1-32. <https://www.springerprofessional.de/en/integrating-artificial-intelligence-with-piezoelectric-nanogener/50980658>
7. Ali, A., Sheeraz, M. A., Bibi, S., Khan, M. Z., Malik, M. S., & Ali, W. (2021). Artificial neural network (ANN)-based optimisation of a numerically analysed m-shaped piezoelectric energy harvester. *Functional Materials Letters*, 14(08), 2151046. https://doi.org/10.1142/S1793604721510462?urlappend=%3Futm_source3Dresearchgate.net26utm_medium3Darticle
8. Selim, K. K., Mostafa, L., & Abdellatif, S. O. (2025). Machine learning-driven optimisation of piezoelectric energy harvesters for low-frequency applications. *Microsystem Technologies*, 117. DOI: <https://dl.acm.org/doi/10.1007/s00542-025-05879-0>
9. Saqib, M., Kaloi, G. S., Gul, M., Nazir, M. S., Koondhar, M. A., Albasha, L., & Alsaif, F. (2025). An Effective AFNIS-MPPT-Based Method for Optimising Hybrid Energy Harvesting Systems. *IEEE Access*. <https://ui.adsabs.harvard.edu/abs/2025IEEAA..1345527S/abstract>
10. Adhikari, S., Friswell, M. A., & Inman, D. J. (2009). Piezoelectric energy harvesting from broadband random vibrations. *Smart materials and structures*, 18(11), 115005. <https://iopscience.iop.org/article/10.1088/09641726/18/11/115005>, works remain significant, see the [declaration](#)
11. Mostafa, M. G., Motakabber, S. M. A., & Ibrahimy, M. I. (2016, July). Design and analysis of a buck-boost converter circuit for a piezoelectric energy harvesting system. In the 2016 International Conference on Computer and Communication Engineering (ICCE) (pp. 204-207). IEEE. <http://irep.iium.edu.my/52277/>

12. Zhang, L., Al-Amoudi, A., & Bai, Y. (2000, September). Real-time maximum power point tracking for grid-connected photovoltaic systems. In 2000 Eighth International Conference on Power Electronics and Variable Speed Drives (IEE Conf. Publ. No. 475) (pp. 124-129). IET.
DOI: <https://doi.org/10.1049/cp:20000232>, works remain significant, see the [declaration](#)
13. Rodriguez, J. C., Nico, V., & Punch, J. (2019, April). Powering wireless sensor nodes for industrial IoT applications using vibration energy harvesting. In 2019, IEEE 5th World Forum on Internet of Things (WF-IoT) (pp. 392-397). IEEE.
DOI: <https://doi.org/10.1109/WF-IoT.2019.8767352>
14. Cai, M., Yang, Z., Cao, J., & Liao, W. H. (2020). Recent advances in human motion have spurred interest in energy harvesting systems for wearables. *Energy Technology*, 8(10), 2000533.
DOI: <https://doi.org/10.1002/ente.202000533>
15. Jiang, X., Li, Y., Li, J., Wang, J., & Yao, J. (2014). Piezoelectric energy harvesting from traffic-induced pavement vibrations. *Journal of Renewable and Sustainable Energy*, 6(4).
DOI: <https://doi.org/10.1063/1.4891169>, works remain significant, see the [declaration](#)
16. Zhou, M., Hara, Y., & Makihara, K. (2025). Model predictive control for optimised piezoelectric energy harvesting under multimodal vibration excitation: theory and simulation. *Engineering Research Express*, 7(2), 025526. <https://iopscience.iop.org/article/10.1088/2631-8695/add083>
17. Sakulkar, P., & Krishnamachari, B. (2017). Online learning schemes for power allocation in energy harvesting communications. *IEEE Transactions on Information Theory*, 64(6), 4610-4628. https://anrg.usc.edu/www/papers/Online_Learning_over_MDPs.
18. lu, T., Chakraborty, C., Yang, F., Lai, X., Alharbi, A. (2024). An energy harvesting algorithm for UAVinyML consumer electronics in low-power IoT *IEEE Transactions on Consumer Electronics*, 70(4),
DOI: <https://dl.acm.org/doi/abs/10.1109/TCE.2024.3419784>

AUTHOR'S PROFILE



Ismail Alazhari Abubaker Bashar Omer is a researcher in Renewable Energy at the University of Blue Nile, Ad-Damazin, Sudan. He holds a strong academic foundation in engineering and sustainable energy systems. His primary research focuses on advancing piezoelectric energy harvesting (PEH) technologies, with a specialisation in developing intelligent control systems. His recent work, as presented in this manuscript, demonstrates the innovative application of Artificial Neural Networks (ANN) for real-time Maximum Power Point Tracking (MPPT). This research directly addresses the critical challenge of dynamic impedance matching to maximise power extraction from ambient vibrations, contributing to more efficient energy solutions for low-power IoT and sensor devices. He is an active contributor to the fields of smart materials and renewable energy, with publications that bridge advanced computational methods and practical power electronics design. His work emphasises the creation of robust, computationally efficient algorithms suitable for deployment in resource-constrained environments.

Disclaimer/Publisher's Note: The statements, opinions and data contained in all publications are solely those of the individual author(s) and contributor(s) and not of the Blue Eyes Intelligence Engineering and Sciences Publication (BEIESP)/ journal and/or the editor(s). The Blue Eyes Intelligence Engineering and Sciences Publication (BEIESP) and/or the editor(s) disclaim responsibility for any injury to people or property resulting from any ideas, methods, instructions, or products referred to in the content.